



HAL
open science

Thermal history of the Sabinas - Piedras Negras Basin (Northeastern Mexico): Insights from 1D modelling

Luis Fernando Camacho-Ortegón, Luis Martínez, Juan Josué Enciso-Cardenas,
Arturo Bueno-Tokunaga, Jacques Pironon, Fernando Núñez-Useche

► To cite this version:

Luis Fernando Camacho-Ortegón, Luis Martínez, Juan Josué Enciso-Cardenas, Arturo Bueno-Tokunaga, Jacques Pironon, et al.. Thermal history of the Sabinas - Piedras Negras Basin (Northeastern Mexico): Insights from 1D modelling. *Journal of South American Earth Sciences*, 2022, 115, pp.103756. 10.1016/j.jsames.2022.103756 . insu-03665911

HAL Id: insu-03665911

<https://insu.hal.science/insu-03665911>

Submitted on 13 Jun 2023

HAL is a multi-disciplinary open access archive for the deposit and dissemination of scientific research documents, whether they are published or not. The documents may come from teaching and research institutions in France or abroad, or from public or private research centers.

L'archive ouverte pluridisciplinaire **HAL**, est destinée au dépôt et à la diffusion de documents scientifiques de niveau recherche, publiés ou non, émanant des établissements d'enseignement et de recherche français ou étrangers, des laboratoires publics ou privés.

Thermal history of the Sabinas - Piedras Negras Basin (Northeastern Mexico): Insights from 1D modelling

Luis Fernando Camacho-Ortegón^{a,*}, Luis Martínez^b, Juan Josué Enciso-Cardenas^a, Arturo Bueno-Tokunaga^a, Jacques Pironon^c, Fernando Núñez-Useche^d

a Centro de Investigación en Geociencias Aplicadas, Universidad Autónoma de Coahuila, Boulevard Simon Bolívar #303A, Nueva Rosita, Coahuila de Zaragoza, C.P. 26830, Mexico

b Université de Strasbourg – CNRS, UMR 7063 - Institut Terre et Environnement de Strasbourg, Ecole et Observatoire des Sciences de La Terre, Equipe GeOLS, Strasbourg, France

c Université de Lorraine, GeoRessources - Campus ARTEM, BP 14234, F-54042, Nancy, France

d Instituto de Geología, Universidad Nacional Autónoma de México, Alcaldía Coyoacán, 04510, Ciudad de México, México

The thermal and burial history of the Sabinas-Piedras Negras basin was studied by 1D modelling using vitrinite reflectance values measured on core samples from nine wells. Three heat flow scenarios led to model calibrations, including a simple one and a complex one integrating a thermal anomaly following the maximal burial phase. The differences in hydrocarbon generation curves due to these two scenarios were studied. The studied thermal anomaly induces two distinct phases of primary cracking of kerogen. The first phase is clearly due to burial, whereas the second seems to be due to the thermal event. The increase in the proportion of converted organic matter attributed to this second phase varies depending on the source rocks considered, e.g., for the La Casita source rock, there is a 10% TR increase, whereas that of the La Peña and Eagle Ford source rocks, is 35 and 15% respectively. The thermal evolution of organic matter in the Sabinas-Piedras Negras Basin is mainly due to the burial phase. In contrast, the thermal event considered only causes a temporal shift of hydrocarbon generation. This hydrocarbon generation, primordial gas, occurred mainly before and during the compressive phase (“late Laramide” time step 40-35 Ma [middle-late Eocene]) that affected the Sabinas-Piedras Negras Basin.

1. Introduction

The Sabinas-Piedras Negras Basin (Coahuila, North-Eastern Mexico) is close to the Gulf of Mexico province (Fig. 1). The Sabinas Basin is considered a maturity hydrocarbons basin, that gas-prone production (Santamaría-Orozco et al., 1991; González-García and Holguín-Quiñones, 1992, 2001; Eguiluz de Antuñano, 2001; Román-Ramos and Holguín-Quiñones, 2001) with an original estimate of recoverable reserves of 766.8 BCF (Eguiluz de Antuñano, 2001). Despite the long history of exploration (in the 1930s) and production (the first productive well was drilled in 1975). Little is known about its thermal and burial history. Many hypotheses were established to explain high maturity levels of observed organic matter (OM) in this basin and its surroundings (e.g., Maverick Basin): hidden batholith-sized magmatic body inducing a regional enhanced heat flow, warm deep basin fluids expulsion (Barker

et al., 2002), or simple burial (Cuevas-Lerée and dissertation, 1985; Eguiluz de Antuñano, 2001) were discussed as possible causes.

Basin modelling has become an essential tool to study sedimentary basins' thermal and burial history and enables the verification of theories on basin evolution. For the Sabinas-Piedras Negras area, only a few studies used this approach, but only taking single wells into account (Santamaría-Orozco et al., 1991). In this paper, nine exploratory wells were studied using a basin modelling approach calibrating heat flow history and erosion to measure vitrinite reflectance as the main kinetic parameter of the maturity. The model results provide an explanation for the maturity levels reached. Hydrocarbon (HC) generation is also examined to determine the timing of hydrocarbon generation. The thermal modelling results, constrained by vitrinite reflectance, consider the maximum burial depth was reached during Paleocene - Eocene ages, taking into account that the youngest preserved rocks are of

* Corresponding author.

E-mail address: luis_camacho@uadec.edu.mx (L.F. Camacho-Ortegón).

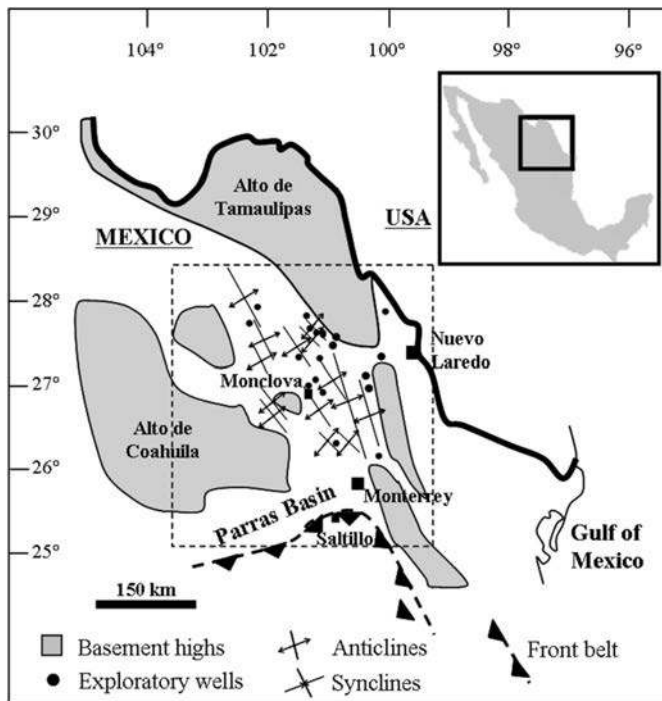


Fig. 1. Location and simplified structural map of the Sabinas - Piedras Negras Basin area. Discontinuous square: location of Fig. 3.

Maastrichtian age in the studied area. The main purposes of this study are: (a) this work aims to model the history of heat flow in the Sabinas Basin, associated with the thermal evolution of vitrinites, geodynamic events, and erosion; (b) investigate whether the evolution of heat flow in the basin influenced the second phase of cracking of organic matter; and (c) test our heat flow hypothesis by modelling the maturation of organic matter compared to what was observed within the Sabinas Basin.

2. Geological setting

The Sabinas-Piedras Negras Basin is located in the North-Eastern of Coahuila, Mexico (Fig. 1). Initially, it developed due to the opening of the proto Gulf of Mexico during the mid-Jurassic (Alfonso, 1978; Longoria, 1984; Wilson, 1990; Santamaría-Orozco et al., 1991; Eguiluz de Antuñano, 2001), which caused the formation of horsts and grabens, including the Sabinas - Piedras Negras basin. This basin may be considered as having evolved as a rift basin in the first part of its history. After this first phase, the Sabinas - Piedras Negras basin underwent decelerating subsidence (Goldhammer and Johnson, 2001). During the Late Cretaceous and Early Tertiary, the basin is assumed to have behaved as a foreland basin during the Laramide orogeny (Goldhammer and Johnson, 2001; Lawton et al., 2001) before inversion. The sedimentary fill reaches a thickness of 5000 m and is mainly Mesozoic, and Santamaría-Orozco et al. (1991) reported a thickness of more than 6000 m in the depocenter. Three super sequences representing five depositional cycles were defined by Santamaría-Orozco et al. (1991), and adjusted by Eguiluz de Antuñano (2001) to describe the evolution of the sedimentary filling in the Sabinas-Piedras Negras Basin. The stratigraphic section for the Sabinas-Piedras Negras Basin is shown in Fig. 2.

The first supersequence is related to the initial rifting phase. It includes La Gloria and Olvido Formations, which were deposited during the Upper Jurassic, and it is mainly composed of conglomerates, salts, and evaporites (Fig. 2). The deposition of this supersequence (Cycle I according to Eguiluz de Antuñano, 2001) occurred principally in a sabkha and coastal marine environment during continuous subsidence (Heim, 1926; Humphrey and Díaz, 1956; Goldhammer et al., 1991; Eguiluz de Antuñano, 2001).

The second supersequence, consisting of cycles II, III, and IV, according to Eguiluz de Antuñano (2001), is related to the thermal subsidence phase and is mainly composed of carbonates evaporites coastal siliciclastic materials deposited from Berriasian to Turonian ages (Fig. 2). According to Eguiluz de Antuñano (2001), this supersequence may be described by three depositional cycles: the first cycle (or cycle II) includes the La Casita and Menchaca - Taraises Formations. The second cycle (or cycle III) comprises the Barril Viejo, Padilla, La Mula, La Virgen, and Cupido Formations. The last depositional cycle (or cycle IV) includes the Cupidito, La Peña, Upper Tamaulipas, Kiamichi, George Town, Del Río, and Buda Formations. The deposition of this supersequence varies from deep marine, neritic, fan-delta, reef, deep basinal to open ramp platform environments on a passive margin (Imlay, 1937; Márquez, 1979; Murillo-Muñetón, 1999; Eguiluz de Antuñano, 2001; Goldhammer and Johnson, 2001).

The last supersequence, or cycle V according to Eguiluz de Antuñano (2001), was deposited in a foreland setting from Turonian to Danian ages and is represented by regressive, terrigenous clastic facies. This supersequence consists of Eagle Ford, Austin, Parras, Upson, San Miguel, Olmos, Escondido Formations, Difunta - Navarro - Taylor, and Midway - Wilcox Groups. This upper age (Danian) is approximate and simply a reference. According to Eguiluz de Antuñano (2001), the 39.5 My B.P. unconformity represents a boundary sequence for this third supersequence, with deep erosion of pre-existing stratigraphic units. The deposits of this supersequence are characterized from ramp-slope, neritic to deltaic environments related to the initial pulses of orogenic uplift to the west (Dumble, 1892; Imlay, 1936; Kelly, 1936; Price and Henry, 1984; Eguiluz de Antuñano, 2001).

3. Structural setting

During the Laramide phase (Late Cretaceous/Early Tertiary), the region underwent an important compression phase, with a regional North-Eastward tectonic transport (Eguiluz de Antuñano, 2001). This phase formed a fold and thrust belt in the eastern region (the Sierra Madre Oriental (SMOr)) and compressive structures in the basin. In the northeastern part of the basin, the deformation was controlled by a high basement. Schematically, the Sabinas-Piedras Negras Basin is represented by narrow anticlines globally-oriented NW/SE, separated by large syncline valleys (Fig. 1). Where Jurassic salt is present, it behaves as a detachment level.

After the Laramide orogeny, a significant stress direction change occurred and decreased horizontal compression. This event could have been affected by the rollback associated with the Farallon Plate (Bird, 2002).

4. Stratigraphic formations of interest

Three main source rock intervals were identified in the Sabinas-Piedras Negras area according to the data supplied by PEMEX (Petroleos Mexicanos Company), and recent petrographic and geochemical studies (Piedad-Sanchez, 2004; Camacho-Ortegón, 2009; Camacho-Ortegón et al., 2017). The most important one is the La Casita Formation (Kimmeridgian - Tithonian), with facies from a neritic to fan-delta complex environment, as was defined by Imlay (1937), after Santamaría-Orozco et al. (1991) made the organic geochemistry analysis. Finally, Eguiluz de Antuñano (2001) and Goldhammer and Johnson (2001) abridged the geologic evolution of this formation. These sediments have high organic carbon content (Total Organic Carbon - TOC), which ranges between 0.5 and 3%, and high organic maturity ($R_p > 2.0\%$). The two other source rocks are La Peña Formation (Late Aptian; 0.4-2.9% TOC; deposited in a deep basinal environment; Imlay, 1936; Humphrey, 1949; Santamaría-Orozco et al., 1991; Eguiluz de Antuñano, 2001; Goldhammer and Johnson, 2001), and Eagle Ford Formation (Turonian; 0.6-2.5% TOC; deposited in a neritic environment; Kelly, 1936; Santamaría-Orozco et al., 1991; Eguiluz de Antuñano, 2001);

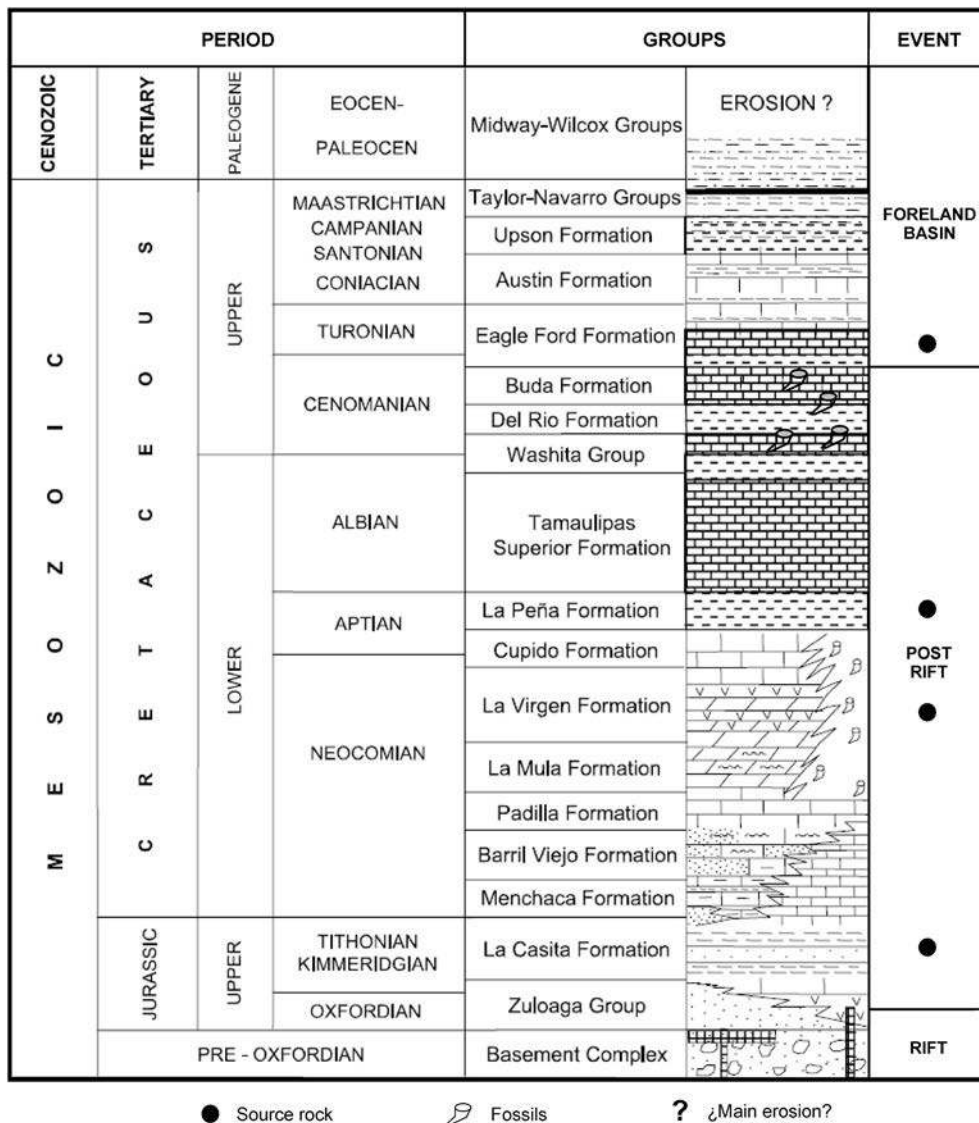


Fig. 2. Stratigraphic section of the Sabinas-Piedras Negras area (Modified from Santamaría-Orozco et al. (1991), and Eguiluz de Antuñano (2001)).

Goldhammer and Johnson, 2001). These three formations mainly contain terrigenous organic matter mixed with low proportions of marine organic matter. Locally, other formations (mainly La Virgen with a facies of sabkha-type lagoonal carbonate environment; Imlay, 1940; Márquez, 1979; Eguiluz de Antuñano, 2001; Goldhammer and Johnson, 2001) may have significant organic matter content (reaching 3.6% TOC). They are then also considered as possible source rocks.

Several reservoir rocks were identified in the Sabinas-Piedras Negras Basin taking into account their geochemical and mechanical characteristics (fracturing, faulting, porosity, permeability, etc.), and their geostatistical modelling (Márquez, 1979; González-García and Holguín-Quiñones, 1992, 2001; Eguiluz de Antuñano, 2001; Román-Ramos and Holguín-Quiñones, 2001). The main reservoir rocks are in the La Gloria (Upper Jurassic), La Casita (Upper Jurassic), Padilla (Hauterivian), La Virgen (Barremian), George Town (Albian), and Austin (Campanian) Formations (Márquez, 1979; Santamaría-Orozco et al., 1991; González-García and Holguín-Quiñones, 1992, 2001; Eguiluz de Antuñano, 2001).

4.1. 1D modelling

One-dimensional modelling of burial history and thermal maturity

was performed on nine gas fields, primarily located in the central area of the basin. The wells' locations are shown in Fig. 3. Computations were performed using the PetroMod 1D software package. Burial history modelling provides the physical framework for thermal and hydrocarbon generation simulation (see a relationship between %R_f and hydrocarbon generation, Table 1). The model was calibrated by modifying the heat flow and erosion until a satisfactory relationship between measured and simulated thermal indicators was observed. The calibration model included mainly the vitrinite reflectance and the wells' bottom temperature, paleobathymetry, and paleotemperature measurements. The software needs massive information as an input data, these are:

4.2. Input parameters

The lithological composition of the different formations was described as mixtures of pure mineralogical end-members. An example of the values considered in this study is given in Table 2 (Camacho-Ortegón, 2009). Refined end-members physical parameters are presented in Table 3.

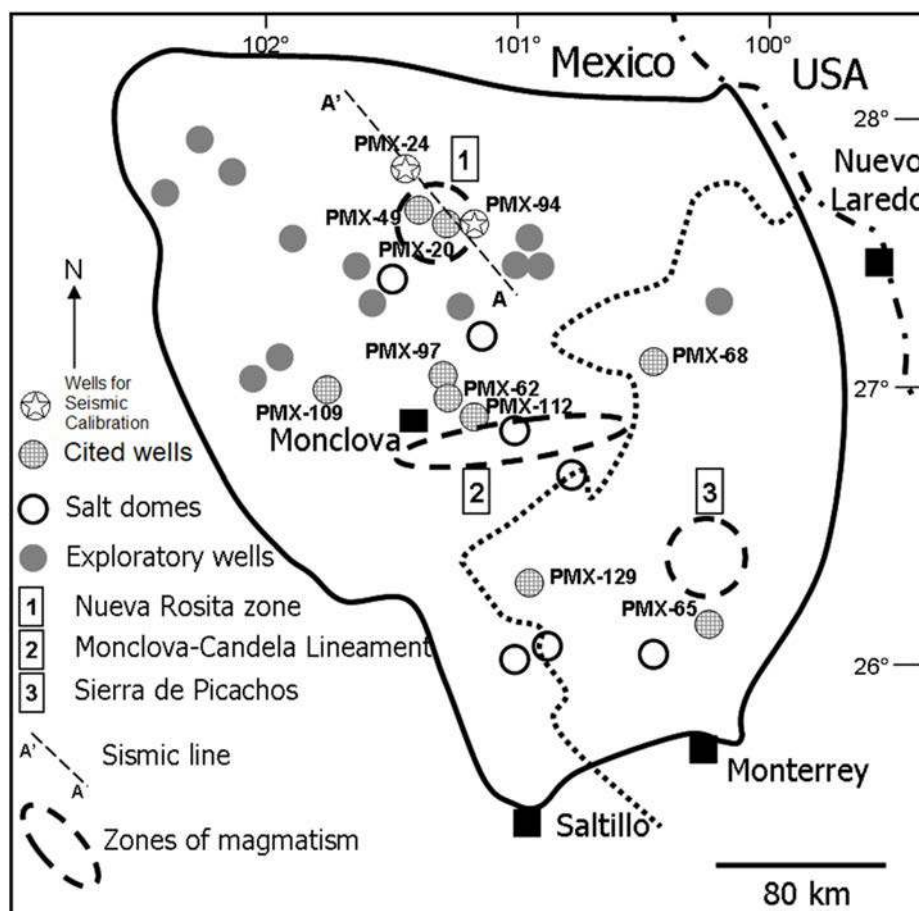


Fig. 3. Location of the studied wells, of the magmatic bodies and salt domes in the Sabinas-Piedras Negras Basin.

Table 1

Easy vitrinite reflectance after Sweeney and Burnham (1990).

%Rr	HC generation
0.25–0.55	Immature
0.55–0.70	Early oil
0.7–1.00	Main oil
1.00–1.30	Late oil
1.30–2.00	Wet gas
2.00–4.00	Dry gas
>4.0	Over mature

4.3. Burial history constraints

The timing of maximum burial and beginning of inversion of the Sabinas-Piedras Negras Basin are not well defined. The youngest preserved sediments in the area of interest are of the Maastrichtian age. In this study, it is considered that the maximum burial depth was reached during Paleocene - Eocene ages and that erosion occurred from these periods until Early Neogene, as postulated by Eguiluz de Antuñano (2001), who used kinematic data and the critical-wedge mechanical model (Dahlen et al., 1984; Davis and Engelder, 1985; Marret and Aranda, 1999). These events are also confirmed by Gray et al. (2001), who utilized K/Ar ages on diagenetic illite, aqueous fluid inclusion homogenization temperatures, apatite fission-track, and U–Th/He periods. The same hypothesis was made when Román-Ramos and Holguín-Quiñones (2001) used biomarkers, vitrinite reflectance, and thermal kinetic modelling for this basin. The chronostratigraphic timescale used to date the different events is from Eguiluz de Antuñano (2001) and Cuevas-Lerée and dissertation (1985).

4.4. Extent of erosion

The most important erosional event occurred in the Early Tertiary. The extent of erosion in the Sabinas-Piedras Negras area is of significant concern because Late Cretaceous and Early Tertiary deposits are preserved only in the eastern part of the study area, reaching a thickness of 2400 m. Nevertheless, deposits and subsequent erosion should have been significantly more significant in the whole area to explain the high maturity levels observed in the basin. Cuevas-Lerée and dissertation (1985), Santamaría-Orozco et al. (1991), Román-Ramos and Holguín-Quiñones (2001) and Camacho-Ortegón (2009) using thermal modelling assumed that ca. 1500–1700 m of sediments were eroded in the Monclova area to explain the high maturity levels. The paleobathymetry data agrees with the sea-level fluctuations in Maastrichtian (Fig. 4; Vail et al., 1977; Haq et al., 1987; Camacho-Ortegón et al., 2017); the calculated erosion is ca. 600–2350 m in the studied area. It seems thus that erosion may be regarded as an essential parameter to be taken into account during simulation. The missing Late Cretaceous - Early Tertiary deposits are assumed to be primarily terrigenous since, during this period, the shoreline migrated eastward (McBride and Caffey, 1979; Goldhammer and Johnson, 2001).

4.5. Thermal constraints

Surface temperatures were considered as having reached a value of ca. 25 °C during the Late Jurassic to Late Cretaceous times before decreasing to the present-day value of ca. 20 °C.

The first step of this thermal study was to define a heat flow evolution curve according to the evolution of the basin. The thermal regime refers to the data provided by Allen and Allen (2005), who estimate the

Table 2

Example of lithological composition considered in this study (after Camacho-Ortegón, 2009).

Formation	Shale	Siltstone	Sandstone	Limestone	Dolomite	Marl	Coal	Evaporite
Wilcox	20	50	30	0	0	0	0	0
Midway	50	20	30	0	0	0	0	0
Mendez	60	40	0	0	0	0	0	0
Navarro	15	10	5	50	0	20	0	0
Taylor	5	10	15	50	0	20	0	0
Escondido	60	20	15	5	0	0	0	0
Olmos	70	10	8	0	0	0	12	0
San Miguel	30	0	70	0	0	0	0	0
Upton Clay	97	0	3	0	0	0	0	0
Austin	30	0	0	50	10	10	0	0
Eagle Ford	40	0	0	60	0	0	0	0
Monclova	0	0	0	100	0	0	0	0
Buda	0	0	0	100	0	0	0	0
Del Río	80	0	0	20	0	0	0	0
G. Town	0	0	0	100	0	0	0	0
Kiamichi	30	10	0	50	0	10	0	0
Mc Knight	30	10	0	50	5	0	0	5
Edwards	5	0	0	70	10	15	0	0
Gleen Rose	50	10	10	10	10	10	0	0
Upper Tamaulipas	5	0	0	80	15	0	0	0
La Peña	30	10	0	40	0	20	0	0
Cupido	10	0	0	70	10	10	0	0
Lower Tamaulipas	0	0	0	80	10	10	0	0
La Virgen	10	10	0	30	5	5	0	40
La Mula	40	10	0	40	0	10	0	0
Padilla	10	0	0	50	40	0	0	0
Taraises	20	10	0	30	0	40	0	0
Barril Viejo	50	10	0	40	0	0	0	0
Menchaca	10	30	0	40	20	0	0	0
La Casita	20	20	40	10	5	0	0	5

Table 3

Main physical parameters considered for modelling.

Lithotype	Density (kg/m ³)	Initial porosity (%)	Compressibility		Thermal conductivity		Heat capacity	
			(Pa ⁻¹)		(W/m K)		(cal/g K)	
			Max	Min	0 °C	100 °C	20 °C	100 °C
Water	1160	0	2	1	0,6	0,68	0,999	1008
Shale	2680	65	60,000	10	1,98	1,91	0,213	0258
Siltstone	2672	56	8000	10	2,14	2,03	0,201	0242
Sandstone	2660	42	500	10	3,12	2,64	0,178	0209
Limestone	2710	42	300	25	2,83	2,56	0,195	0223
Dolomite	2836	30	250	10	3,81	3,21	0,202	0229
Marl	2687	47	940	10	2,23	2,11	0,208	0248
Coal	2000	52	130,000	10	0,5	0,46	0,204	0248
Evaporite	2540	10	60,000	10	4,69	3,91	0,194	0210
Organic matter	1100	0	50,000	10	0,5	0,45	0,200	0240

range of surface heat flow of different types of basins. Consequently, heat flow was considered high during the initial rift phase (ca. 100 mW/m²) and decreased to lower values (between 40 and 65 mW/m²) during the thermal subsidence phase.

During the compressive phase (“late Laramide” time step 40-35 Ma [middle-late Eocene]; Bird, 2002), the average heat flow value was described referring to other studies. The average heat flow value during the foreland phase in the North Alpine Foreland basin is assumed to be close to 60 mW/m² by Schegg et al. (1999) and lower than 55 mW/m² during the compressive phase by Sachsenhofer (2001). In a compressive setting, Gonçalves et al. (2002) estimate heat flow values of ca 40 mW/m². Considering the above, we infer that one value of 60 mW/m² is a maximum value for the Sabinas-Piedras Negras area during the foreland phase. These estimations lead to the evolution curve called scenario one (Fig. 5).

4.6. Thermal indicators

Thermal history reconstruction is based on random vitrinite

reflectance measurements (R_r). R_r remains the most commonly used thermal indicator in thermal modelling (Handhal and Mahdi, 2016). Vitrinite reflectance is a percentage measure of the incident light reflected from the surface of vitrinite particles in sedimentary rock (Beaumont and Foster, 1999). It is termed as % R_o . It is optical parameters symbolized by VR or R_o (reflectance in oil) (Tissot and Welte, 1984). Vitrinite is a coalification product of humic substances originating from the lignin and cellulose of plant cell walls (Taylor et al., 1998).

The relationship between % R_r and hydrocarbon generation depends on the vitrinite’s and the kerogen’s chemistry (Beaumont and Foster, 1999). Sweeney and Burnham (1990) evaluated a simple model of R_r (see EASY% R_o) based on chemical kinetics due to changes in vitrinite composition with time and temperature (Table 1).

The simplified model EASY% R_o uses an Arrhenius first-order parallel-reaction approach with a distribution of activation energies. With EASY% R_o , a vitrinite reflectance vs. time profile can be obtained for a given stratigraphic level if the time-temperature history for that level has been estimated. When applied to multiple stratigraphic levels, EASY

Paleobathymetry in Sabinas-Piedras Negras Basin

Formation	Age (Ma)		Paleobathymetry (m)	
La Casita	142	149	140	116
Padilla	126	130	0	139
La Virgen	121	125	114	64
La Peña	112	119	110	143
Eagle Ford	89	93.5	234	243
Olmos	67	71.3	162	210

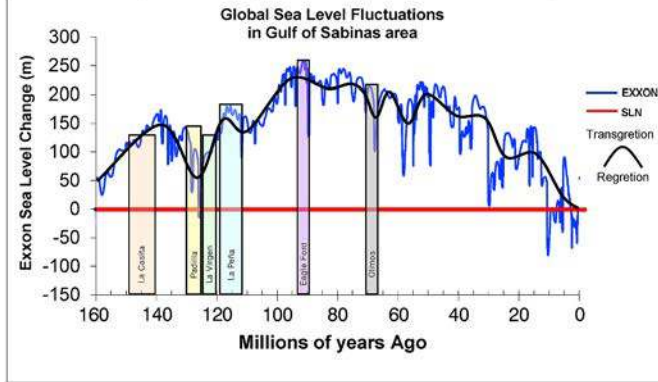


Fig. 4. Chronology of fluctuating Sea Level events in the Gulf of Sabinas and paleobathymetry in the Sabinas-Piedras Negras Basin (EXXON curve data; Vail et al., 1977; Haq et al., 1987; modified after Camacho-Ortegón, 2009). Black line; paleobathymetry Sabinas-Piedras Negras Basin. Blu line; EXXON curve. Redline; Sea Level now (SLN).

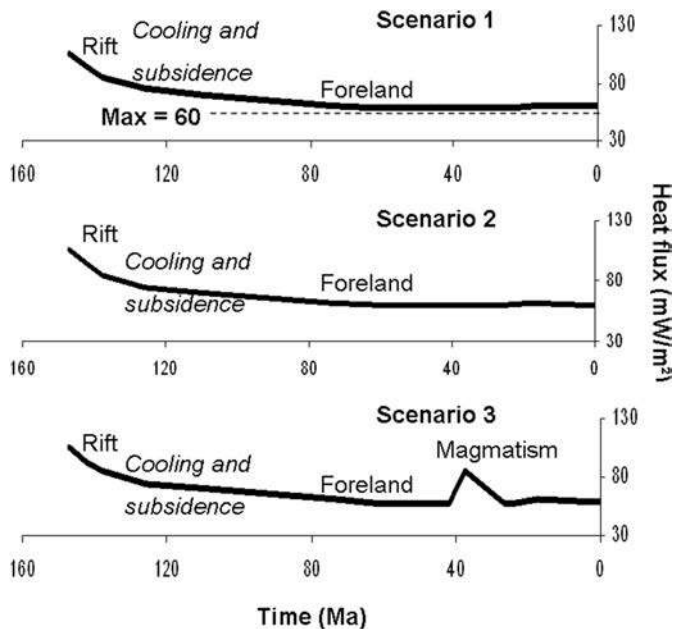


Fig. 5. Heat flow scenarios considered in the thermal reconstruction of the Sabinas-Piedras Negras Basin.

%Ro can be used to compute profiles of the percent of vitrinite reflectance with depth for comparison with borehole data and optimize thermal history models. EASY%Ro successfully estimates vitrinite reflectance due to the thermal metamorphism of sedimentary rocks heated by igneous intrusions, geothermal fluids, and burial in various basin settings (Sweeney and Burnham, 1990).

Measurements complemented the R_f data provided by PEMEX and additional studies (Camacho-Ortegón, 2009) on samples from nine wells made following the established norm ISO 7404-5 (1994). When the organic matter particles were scarce, the recommendations proposed by

Bertrand and Pradier (1993), Barker (1996), and Taylor et al. (1998) were followed. Measurements were performed mainly on source rock samples (i.e., Eagle Ford, La Peña, La Virgen, and La Casita Formations). Measured R_f values are similar to those given by Santamaría-Orozco et al. (1991), González-García and Holguín-Quñones (1992, 2001), and Román-Ramos and Holguín-Quñones (2001), and give values higher than 0.6% for the Eagle Ford Formation, between 0.8 and 1.1% for La Peña, and higher than 2% for La Casita. Thermal history was reconstructed based on these parameters. The bottom temperature of some wells was used to compare the thermal history in 1D modelling.

5. Results

5.1. Present-day thermal regime

The present-day heat flow values were determined using the temperature profiles available for different wells. The discrepancy between the simulated profile and the measured temperatures is moderate (2–3 °C of difference). This result may be considered good (Demongodin et al., 1991). The present-day heat flow values obtained range between 50 and 68 mW/m². These values support the heat flow values given by Bird (1992) and Ritzwoller and Shapiro (2001).

The present-day heat flow map (Fig. 6) established with the results obtained shows that heat flow is more significant in the center of the basin and decreases westward toward the margin of the basin. It also appears that the highest heat flow values are reached in the north of the basin.

5.2. Thermal history

R_f profiles were simulated using the LLNL Easy%Ro algorithm (Sweeney and Burnham, 1990). As a starting point, calculations were performed considering the hypotheses on erosion and heat flow variation during burial history (scenario 1; Fig. 5).

A good match is obtained for the PMX-129 well, considering a heat flow value of 53 mW/m² reached during the maximum burial phase. Nevertheless, for the other wells, it appears that the best matches are obtained considering heat flow values higher than 60 mW/m² at a full

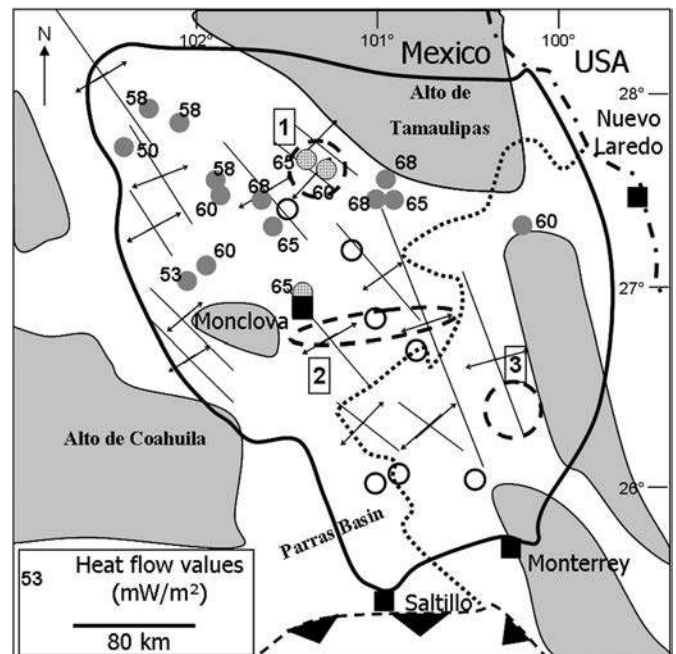


Fig. 6. Present-day heat flow distribution across the basin. Legend is given in Fig. 1 and 3.

burial. Keeping the heat flow under 60 mW/m^2 leads to defective calibration (Fig. 7). It, therefore, appears necessary to project the heat flow value higher when the maximum burial phase occurs.

As for the initial heat flow scenario, assuming a maximum heat flow value of 60 mW/m^2 does not lead to a meaningful calibration with the wells, two additional heat flow scenarios were defined: a first one (scenario 2; Fig. 5), more straightforward than the first one, as it considers no heat flow limit in its variation during the evolution of the basin, and a second additional heat flow scenario (scenario 3; Fig. 5), slightly more complex than the first scenario: heat flow values are kept moderate ($<60 \text{ mW/m}^2$) during the compressive phase, but a thermal anomaly is considered during the Tertiary (Bird, 2002; Ewing, 2003; Chávez-Cabello et al., 2009), after the beginning of the basin inversion. This thermal anomaly appears to be related to the intense magmatic activity observed in the Gulf of Mexico Province, known as the Eastern Alkaline Province (Bloomfield and Cepeda-Dávila, 1973). In the Sabinas area, three magmatic complexes are observed: the Nueva Rosita zone, the Monclova-Candela lineament and the Sierra de Picachos complex (see Fig. 3 for location). The origin of magmatism is currently interpreted in terms of two different tectonic environments: the Monclova-Candela lineament seems to be due to subduction tectonic (Clark et al., 1982; Morton-Bermea, 1995, 1997), whereas the rhyolitic nature of the Sierra de Picachos complex or other structures located close to the basin (see González-Partida et al., 2003) suggests a continental rift origin (Morton-Bermea, 1995, 1997). The age of magmatism is estimated to ca 30 to 45 Ma for the subduction-related magmatism (Clark et al., 1982; Price and Henry, 1984; Chávez-Cabello et al., 2009), but magmatism due to continental rifting appears to be younger (30–32 Ma, Price and Henry, 1984) and temporally related to the extension phase already described (e.g., Bird, 2002). These geodynamical events could have induced a significant heat flow increase, explaining the maturity trends observed in the basin. In the model, this thermal event was considered at 38 Ma.

The results obtained for these two additional scenarios are similar, as no limit is given to the heat flow value (resulting calibration curves are presented in Figs. 7 and 8). It appears quite difficult to rule out one of the two scenarios.

5.3. Effect of the uncertainty of different parameters on calibration curves

This section does not deal with the impact of the flow scenarios, as discussed earlier, but deals with other parameters, such as heat flow, erosion, or physical parameters (thermal conductivity).

Two tests were performed on the different wells, using the PetroRisk module integrated into PetroMod 1D Version 10. This module enables uncertainties to be defined and quantify these uncertainties' effect on the final results.

The first test concerns the effect of heat flow and erosion on the calibration curves. These parameters were increased and decreased in a $\pm 10\%$ interval. The resulting curves show an imperfect pattern for the minimum and maximum calibration curves (Fig. 9A), indicating thus that this interval may be considered the confidence interval.

Another test was performed to determine the effect of the thermal conductivity of the different formations on the calibration curves. For all the tested formations, thermal conductivity was considered to vary within a $\pm 20\%$ interval. The resulting curves (Fig. 9B) show that the effect of an essential uncertainty of thermal conductivity is negligible regarding the impact of heat flow and erosion variations.

This observation is confirmed by the third Test results, which integrate the three parameters types (erosion, heat flow, and thermal conductivity). The resulting curve (Fig. 9C) is similar to the curve observed when only heat flow and erosion variations are considered (Fig. 9A). Thus, it may be assumed that the values (erosion and heat flow) determined in this study have a margin of error lower than 10% and that the uncertainty of the physical parameters is of minor influence.

6. Discussion

6.1. Thermal and burial history

Regarding the distribution of the eroded thickness estimated from R_r profiles (Fig. 8), it seems that the distribution of the deposits is more significant in the south (PMX-129 well, estimated original deposit thickness = 3500 m) than in the center of the basin, where estimated deposit thickness reaches 2100–2500 m. In the same way, an eastward decrease of the considered deposit amount in the calculations is

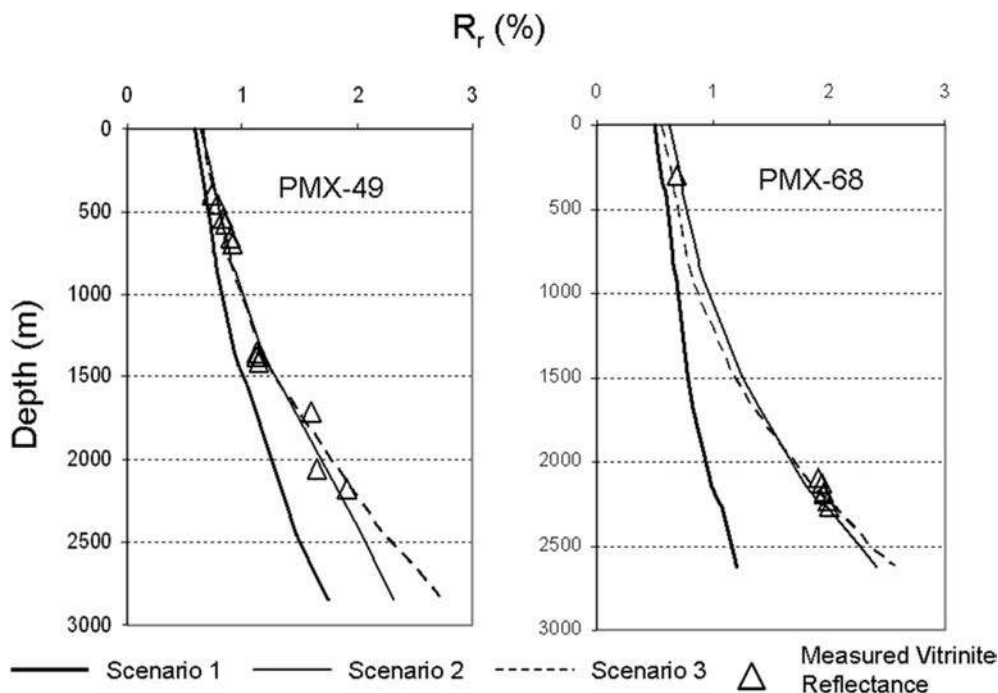


Fig. 7. Example of R_r profiles simulated considering scenarios and measured values for two wells.

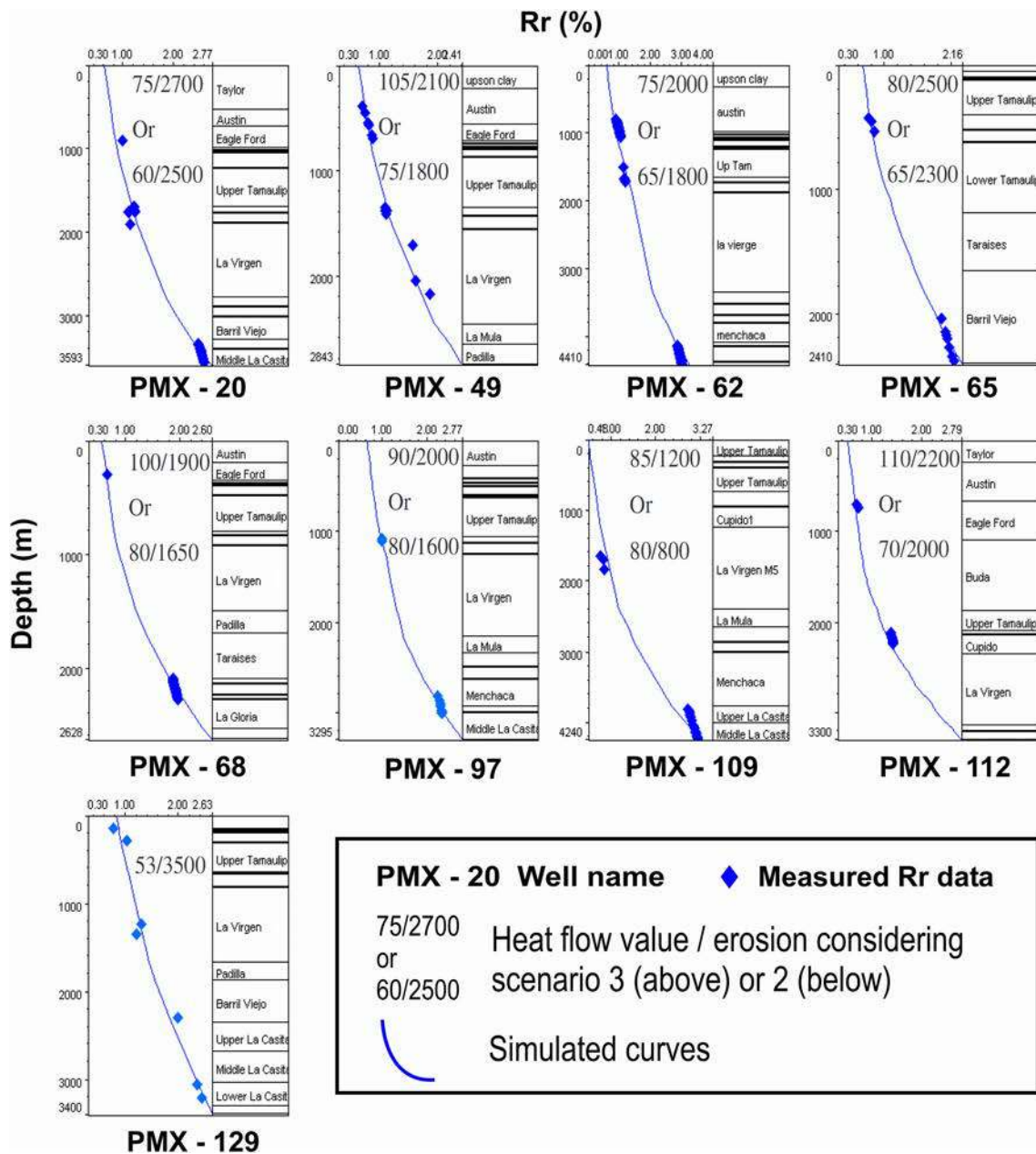


Fig. 8. Calibration results for the different wells. See Fig. 3 for the location of the wells.

observed.

In the south of the Sabinas - Piedras Negras basin (PMX-129 well), the difference between present-day temperature calculated assuming a present-day heat flow of ca. 60 mW/m² and maximum paleotemperature of burial (i.e., the highest temperature reached during burial) is ca. 120 °C. This value is slightly lower than values estimated from the curves obtained by Gray et al. (2001) for the La Popa Basin, with average values between 140 and 155 °C close to the front belt.

Therefore, it would appear that, in the Sabinas - Piedras Negras Basin, maximum erosion occurs close to the front belt of the SMOr and decreases with increasing distance from this limit.

Fig. 10 shows the PetroMod 1D models by nine studied wells (PMX-20, 49, 62, 65, 68, 97, 109, 112, and 129), and estimated burial history curve, overlay with oil, and gas window, isoline to temperature evolution, erosion, the timing of hydrocarbon generation in a systematic relationship by vitrinite reflectance maturity data (Fig. 8).

6.2. Lateral distribution of heat flow values and influence of salt structures

Heat flow anomalies calculated considering scenario three are mainly located in the northern part of the basin (Fig. 11), where most of the magmatic bodies were identified. Heat flow values associated with the thermal event vary from 100 to 75 mW/m² for wells, separated by a short distance, and therefore, they have a significant variation. Considering that some wells may be directly affected by heating due to the intrusions, these differences may be explained.

Salt domes were also observed in the Sabinas-Piedras Negras basin (Eguiluz de Antuñano, 2001). Salt has a very high thermal conductivity and can modify the temperature distribution in sedimentary basins (e.g., Mello et al., 1995). Fig. 11 shows the distribution of salt domes and estimated heat flow during the thermal event. Note that there is no systematic relationship between thermal anomalies and the distribution of salt domes. This implies that salt does not influence observed vitrinite

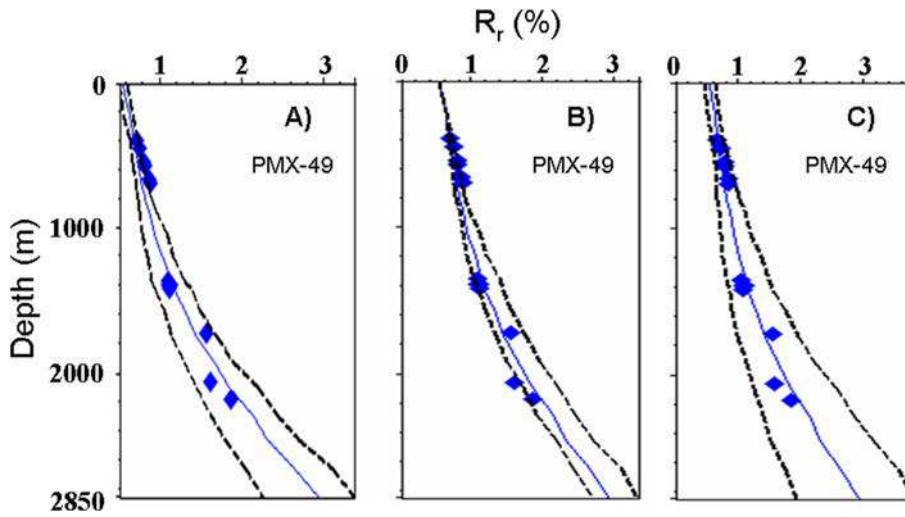


Fig. 9. Calibration interval obtained considering margin error on heat flow and erosion (A) and thermal conductivity (B), and the three parameters (C).

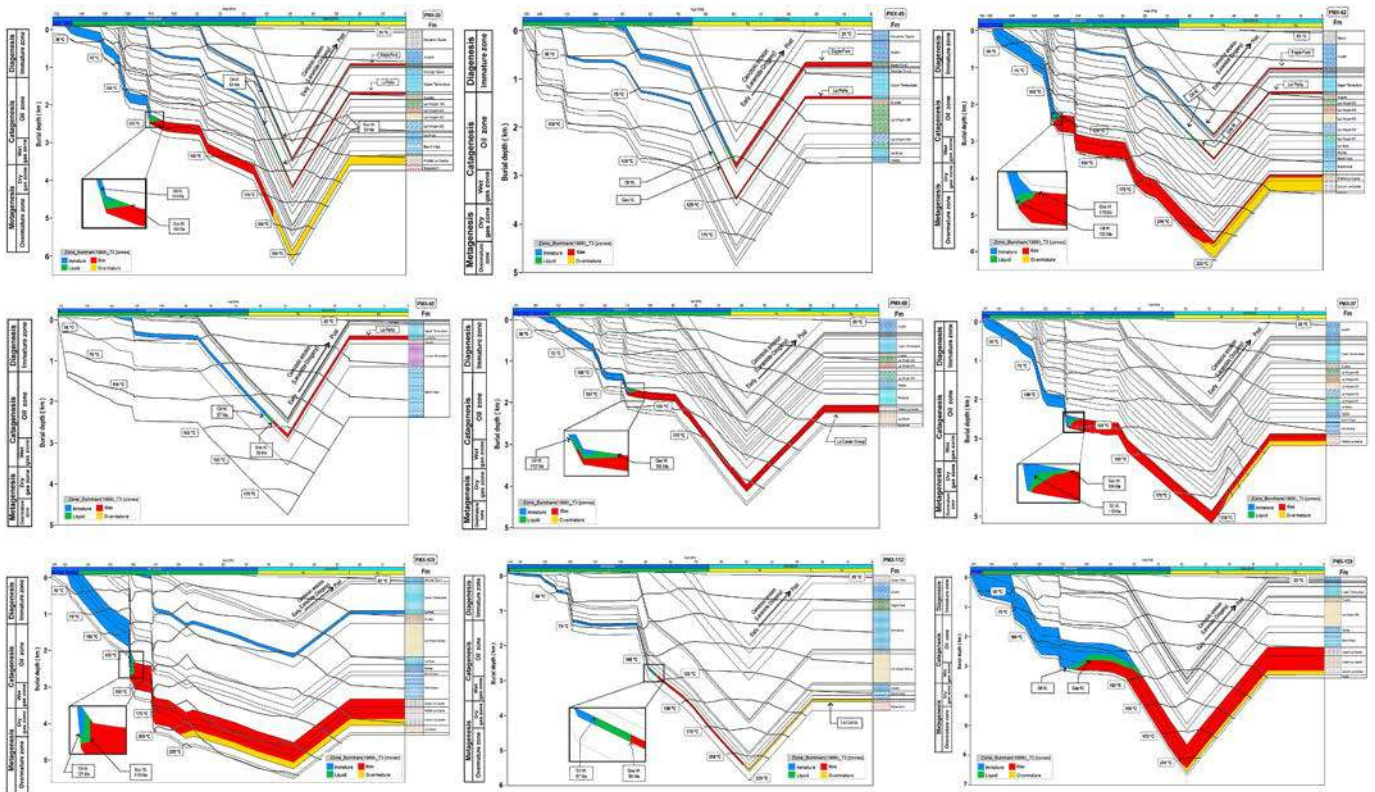


Fig. 10. Burial history for nine well's in the Sabinas-Piedras Negras Basin. The results mainly indicate a gas-prone potential agreeing with the current HC production.

reflectance and temporal heat flow variations.

6.3. Effect of the thermal anomaly on hydrocarbon generation

Hydrocarbon generation was simulated in this study for the selected source rocks. Kerogen cracking may be simulated using different models (Bouster et al., 1980; Braun and Burnham, 1992; Burnham et al., 1996) such as T_{max} -shift, serial first-order reaction, Bouster four-parameter, or three-parameter nucleation. However, it is commonly simulated assuming parallel reactions described with a single pre-exponential factor and a discrete or continuous distribution of activation energies (e.g., Ungerer and Pelet, 1987; Pepper and Corvi, 1995; Vandembroucke

et al., 1999).

As shown previously, primary source rocks in this basin are mixtures of type II and III organic matter; currently available models deal with pure source rocks only, making it necessary to find a compromise. As type III organic matter is dominant in these three formations, only terrigenous organic matter is considered in this study. As no immature OM sample was available, simulations were performed using a default type III OM kinetic model because the La Casita Formation has this type of organic matter. The kinetic model used is the LLNL Type III model (Burnham, 1989). This choice has no influence, as the aim of these simulations is not to evaluate the hydrocarbon potential of the basin but to test the relative effect of different heat flow scenarios on generation

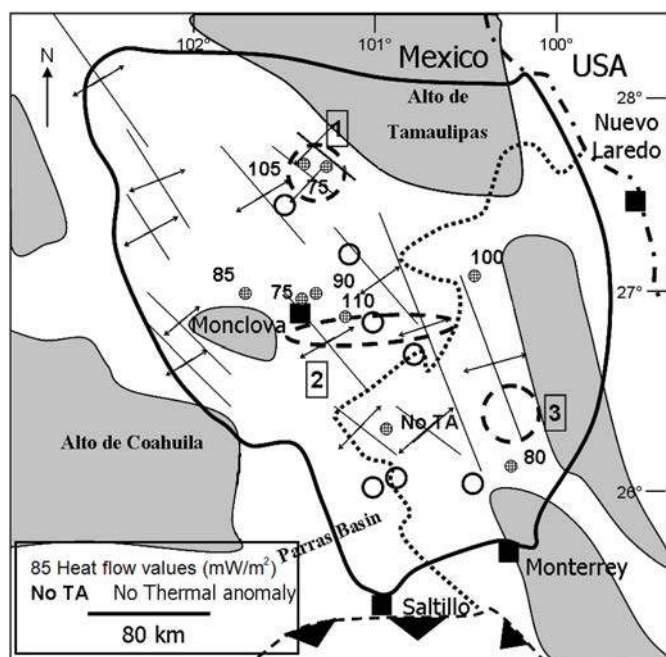


Fig. 11. Calculated heat flow values associated with the thermal event. Legend is given in Figs. 1 and 3.

curves.

Transformation ratio (TR) evolution was simulated considering the thermal field calculated using the two different heat flow scenarios considered possible (scenarios 2 and 3). These two thermal histories induce different shapes of TR evolution curves (Fig. 12).

CONSIDERING SCENARIO TWO, the HC generation curves show a continuous evolution curve, as the thermal field is mainly controlled by burial. Scenario three, integrating a thermal anomaly, induces a temporal shift of TR evolution curves. This delay is significantly more significant for the shallowest source rocks than the deepest (the La Casita Formation).

The thermal anomaly has another effect on TR evolution curves: it induces two distinct phases of primary cracking of kerogen. The first phase is clearly due to burial, whereas the second seems to be due to the thermal event. The increase in the proportion of converted OM attributed to this second phase varies depending on the source rocks considered. For the La Casita source rock, there is a 10% TR increase, whereas that of the La Peña and Eagle Ford source rocks is 35 and 15%, respectively.

This delay in HC generation due to the thermal event does not imply any considerable variation in the distribution of HC generated, as most of the generation occurs when maximum burial is reached. However, as explained earlier, the assumption that a thermal event induced the secondary cracking of primary components entirely agrees with petrographic observations. The generation of gas by secondary cracking should be considered when estimating the Sabinas-Piedras Negras gas potential.

Based on these results, it appears that hydrocarbon generation occurred mainly before and during the compressive phase that affected the Sabinas - Piedras Negras basin. Assuming that the folding occurred during this phase of compression and taking into account the reported data by Santamaría-Orozco et al. (1991), González-García and Holguín-Quiñones (1992, 2001), Eguiluz de Antuñano (2001), Gray et al. (2001), and Román-Ramos and Holguín-Quiñones (2001), hydrocarbon traps formed while most of the hydrocarbons were generated (Fig. 13). Nevertheless, a complete study would be necessary to determine if the hypothesis of a thermal event could induce differences in modelling integrating hydrocarbon migration.

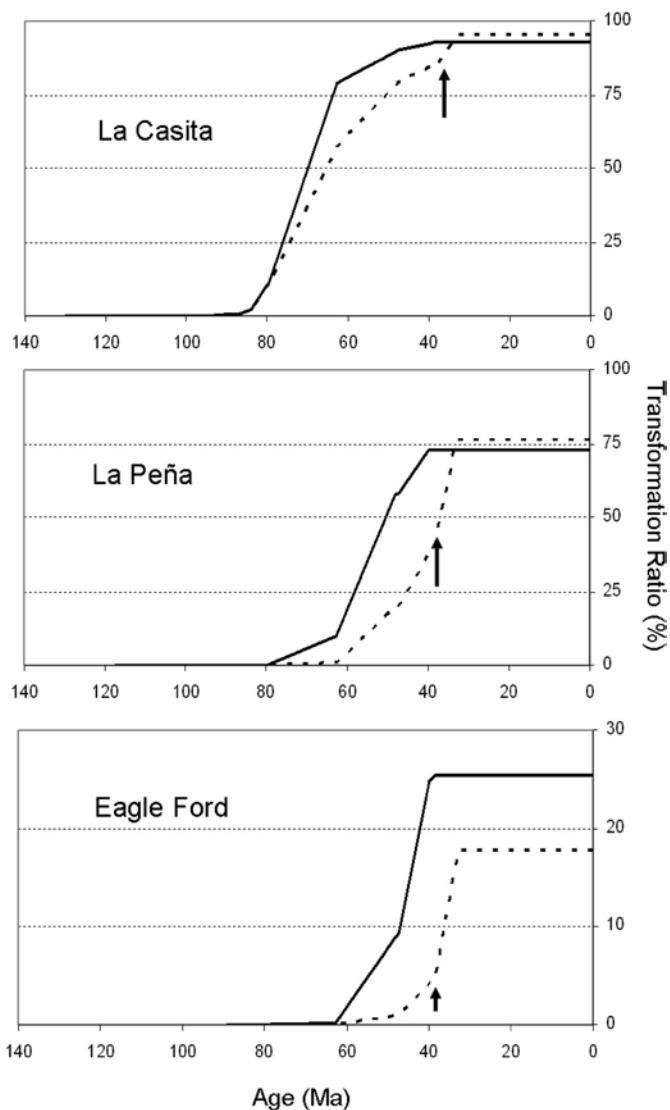


Fig. 12. The vertical scale of the Eagle Ford Formation, whose bottom does not surpass the 1000 m in depth at the Sabinas-Piedras Negras Basin, is exaggerated to show the TR trend. Considering scenarios 2 (continuous line) and 3 (dashed line), transformation ratio evolution curves were calculated for the three primary sources of rocks. Black arrows: thermal anomaly.

6.4. Preferred heat flow scenario

From the results obtained considering either scenario two or three, it appears challenging to rule out one of the two scenarios. Nevertheless, tectonic events such as subduction and extension are expected to induce significant increases in local heat flow, more so if magmatism is associated. This would be the first argument in favor of scenario 3.

Another argument is carried out by the petrographic study of the basin (Piedad-Sanchez, 2004; Camacho-Ortegón, 2009). Different types of bitumen and pyrobitumen were observed during the petrographic analysis of the Sabinas-Piedras Negras basin. Devolatilization vacuoles, porosity, and fracturing were also observed in macerals and could be interpreted as evidence of secondary cracking (Van Balen et al., 2000; Zeman et al., 2000; Wan Hasiyah, 2001; Martínez et al., 2002). Different thermal events explained these observations.

USING SCENARIO THREE, the HC generation was simulated and reconstructed oil and gas generation from a source rock, migration, and accumulation with PetroMod 2D package (see the tutorial by modelling methods with Flowpath, Darcy, Invasion Percolation, and Hybrid

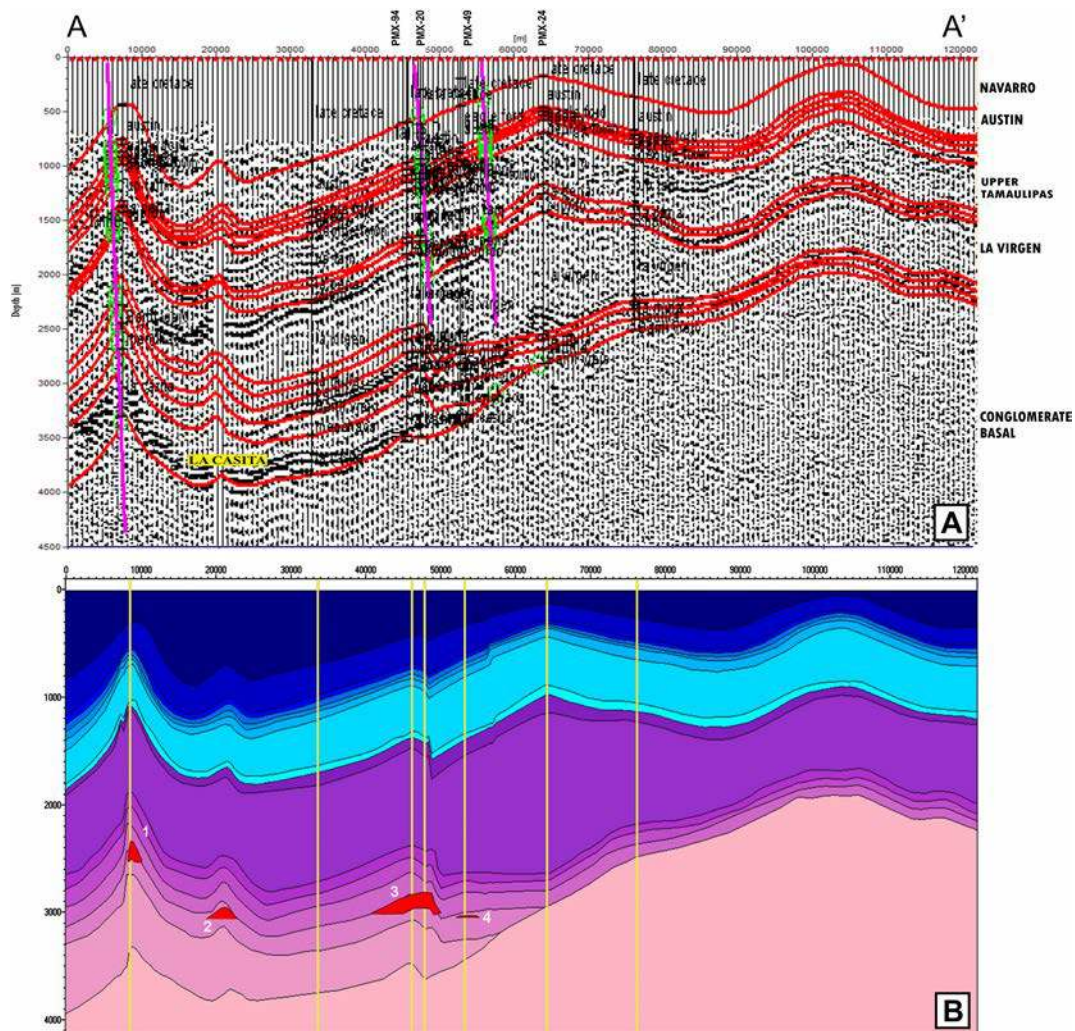


Fig. 13. Cross-section on a seismic line in the Sabinas-Piedras Negras Basin (A). Location of the cross-section in Fig. 3 (A-A'). The simulation of the HC generation with PetroMod shows mainly four gas accumulations in section A-A' with a total of $\sim 154 \text{ Mm}^3$ of dry gas. Interpreted section for seismic sequence analysis in the study area (B). Currently, the PMX-20, PMX-49, and PMX-94 wells have gas production. Distances and depth are in meters.

(Darcy + Flowpath) technology [Petromod 2D tutorial, 2007], on the seismic line A-A' for the Sabinas-Piedras Negras Basin (Fig. 13A). Cautiously, the modelling results confirm the studied basin like a gas-prone basin, showing mainly four gas accumulations in regional 2D cross-section (results from the 2D modelling to section A-A') equivalent of $\sim 154 \text{ Mm}^3$ of dry gas (Fig. 13B). These cautious predictions agree with the defined four gas reservoirs (Fig. 13B; 1 to 4), mainly in the PMX-20 well with a reasonable gas production rate.

6.5. Relationship between %Rr and maximum fluid inclusions temperature

The fluid inclusion microthermometric analyses have been used successfully in the petroleum exploration industry (e.g., Bodnar and Vityk, 1994; Pironon, 2004 and others) for estimating the temperatures, timing, and pore fluid origins of various diagenetic minerals in sources and reservoir rocks (e.g., Roedder, 1984; Walderhaug, 1990). Tobin and Claxton (2000) established fluid inclusion microthermometry from a new inorganic thermal maturity tool that can help fill the void in geologic and sampling limitations. This tool uses an empirical calibration of fluid inclusion data and vitrinite reflectance data to estimate thermal maturity (Fig. 14). Currently, the models that relate the %Rr with the homogenization temperature (Th) of fluid inclusions allow the model to approach a more acceptable thermal calibration (Barker and

Pawlewicz, 1986; Barker and Goldstein, 1990). This correlation technique (Barker and Pawlewicz, 1986; Tobin and Claxton, 2000) is beneficial in basins with no macerals (Bourdet et al., 2010; Blaise et al., 2014), which helps users to accurately convert Th data to vitrinite reflectance equivalents (%Rr equivalent) in thermal maturity studies.

In conclusion, the latest techniques conventional in organic maturity (e.g., Sweeney and Burnham, 1990; ISO 7404-3, 1994; ISO 7404-5, 1994) have proven to be effective in determining the evolution of diagenesis in sedimentary series and optimizing basin models in the last 50 years.

Finally, Sabinas Piedras Negras Basin is suitable for applying the Tobin and Claxton (2000) tool since it would allow a more detailed evaluation of the evolution of the heat flux in a larger area than that represented in this work, considering a new Th study in outcrops from the Popa Basin to the Alto de Tamaulipas area, contributing further information to the regional tectonic, thermal anomaly and diagenetic history.

7. Conclusion

During the basin modelling study performed on the Sabinas Piedras Negras basin, three heat flow scenarios led to similar calibration results, and it appears difficult to rule out either one.

Hydrocarbon generation curves were simulated considering these

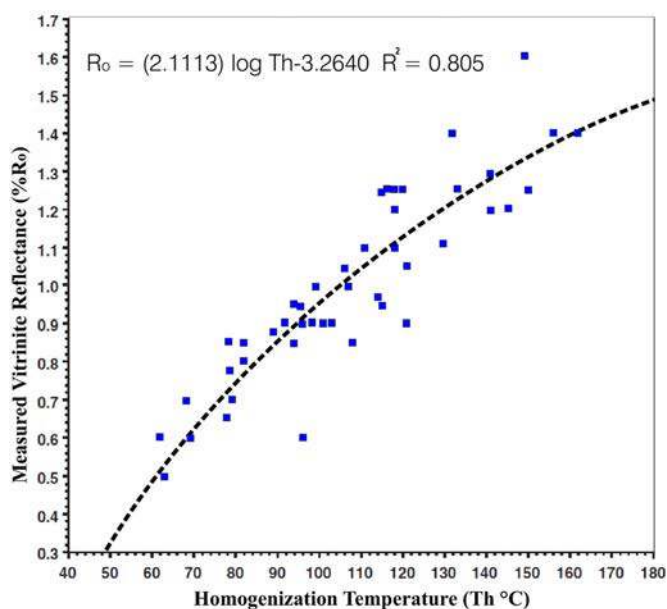


Fig. 14. Logarithmic Crossplot of vitrinite reflectance data (% Ro) vs. homogenization temperature of fluid inclusion Th (°C), a new inorganic thermal maturity tool for estimating thermal maturity values (VR equivalents) from fluid inclusion data that capitalizes on the tendency of aqueous inclusions in calcite to reequilibrate during burial overheating. (modified after Tobin and Claxton, 2000).

two possible scenarios. The differences between the two curves show that this thermal event would not have induced a critical secondary cracking phase. Most organic matter evolution would have occurred when full burial was reached.

Geodynamic considerations and, more importantly, a previous petrographic study would favor the hypothesis of a thermal anomaly occurring after the burial phase.

The results of this modelling approach for the Sabinas-Piedras Negras basin confirm an OM with a high maturity level. Apparently, in the north of the basin, a thermal anomaly can be delineated and should be considered for the HC evaluation in the basin.

Considering the constraints for modelling the regional 2D cross-section of the study area showing the simulation of HC generation for a seismic line indicates potential accumulation to 154 Mm³ of dry gas. The gas accumulations coincide with some defined reservoirs through the gas producer.

Each exploratory well may calculate the local erosion and heat flow to improve the results of this modelling in the Sabinas-Piedras Negras Basin. New geological data of other wells (e.g., fluid inclusions, 3D seismic, isotopes, and other geochemical and petrographic data.) in the basin are indispensable to locate new reservoirs and quantify HC reserves with the best precision in this prone gas basin.

CRediT authorship contribution statement

Luis Fernando Camacho-Ortegón: Methodology, Investigation. **Luis Martínez:** Software. **Juan José Enciso-Cardenas:** Investigation. **Arturo Bueno-Tokunaga:** Data curation. **Jacques Pironon:** Investigation. **Fernando Núñez-Useche:** Writing – review & editing.

Declaration of competing interest

The authors declare that they have no known competing financial interests or personal relationships that could have appeared to influence the work reported in this paper.

Acknowledgments

The authors express their gratitude to Exploration and Production - North Region - Petróleos Mexicanos (PEMEX, Mexico), for providing data and permission for publishing this manuscript. The authors are also indebted to the Centro de Investigación en Geociencias Aplicadas (CIGA-UAdeC, México), INCAR-CSIC (Oviedo, Spain), and GeoResources lab Université de Lorraine (Nancy, France) for help with the analyses. The authors are also indebted to the IES, Germany support team for helpful technical support. R.F. Sachsenhofer is gratefully acknowledged for his helpful comments. The authors offer special thanks to the reviewers of this article, especially to Ph. D. Francisco J. Vega and Ph.D. Claudio Bartolini for his suggestions.

References

- Allen, P.A., Allen, J.R., 2005. Basin Analysis: Principles and Applications. Blackwell Publishing, Scientific Publications, p. 549.
- Alfonso, Z.J., 1978. Geología regional del sistema sedimentario Cupido. Bol. Asoc. Mex. Geol. Pet. 30, 1–56. http://publicaciones.amgp.org/administrativo/publicaciones/archivos/portada/5dae80a72e4a4.1978_Ene_Jun_012.pdf.
- Barker, ChE., Pawlewicz, M.J., 1986. The correlation of vitrinite reflectance with maximum temperature in humic organic matter. Lecture Notes in Earth Sciences. In: Buntebarth, G., Stegena, L. (Eds.), Palaeogeothermics. Edited by, vol. 5. Springer-Verlag Berlin Heidelberg, pp. 79–93.
- Barker, ChE., Goldstein, R.H., 1990. Fluid-inclusion technique for determining maximum temperature in calcite and its comparison to the vitrinite reflectance geothermometer. Geology 18, 1003–1006. [https://doi.org/10.1130/0091-7613\(1990\)018<1003:FITFDM>2.3.CO;2](https://doi.org/10.1130/0091-7613(1990)018<1003:FITFDM>2.3.CO;2).
- Barker, ChE., 1996. A comparison of vitrinite reflectance measurements made on whole-rock and dispersed organic matter concentrate mounts. Org. Geochem. 24 (2), 251–256. [https://doi.org/10.1016/0146-6380\(96\)00022-8](https://doi.org/10.1016/0146-6380(96)00022-8).
- Barker, ChE., Warwick, P.D., Gose, M., Scott, R.J., Klein, J.M., Hook, R.W., 2002. The sacatosa coalbed methane field: a first for Texas. In: AAPG Annual Meeting. March 10–13, Houston, Texas.
- Baumont, E.A., Foster, N.H., 1999. Treatise of petroleum geology/handbook of petroleum geology: exploring for oil and gas traps. In: Chapter 6: evaluating source rocks, by Carol A. Law. The American Association of Petroleum Geologists. <https://doi.org/10.1306/TrHbk624.V3>.
- Bertrand, P., Pradier, B., 1993. Optical methods applied to source rock study. In: Bordenave, M.L. (Ed.), Applied Petroleum Geochemistry. Technip, Paris, pp. 281–310.
- Bird, P., 1992. Deformation and uplift of north America in the Cenozoic era. In: Billingsley, K.R., Brown III, H.U., Derohanes, E. (Eds.), Scientific Excellence in Supercomputing. The IBM 1990 Contest Prize Papers, vol. 1. Baldwin Press, Athens, Georgia, pp. 67–105.
- Bird, P., 2002. Stress direction history of the western United States and Mexico since 85 Ma. Tectonics 21 (3), 1–12. <https://doi.org/10.1029/2001TC001319>.
- Blaise, Th., Barbarand, J., Kars, M., Ploquin, F., Charles, A., et al., 2014. Reconstruction of low temperature (<100 °C) burial in sedimentary basins: A comparison of geothermometer in the intracontinental Paris Basin. Mar. Petrol. Geol. 53, 71–87. <https://doi.org/10.1016/j.marpetgeo.2013.08.019>.
- Bloomfield, K., Cepeda-Davila, L., 1973. Oligocene alkaline igneous activity in NE Mexico. Geol. Mag. 110 (6), 551–555. <https://doi.org/10.1017/S0016756800037948>.
- Braun, R.L., Burnham, A.K., 1992. PMOD: a flexible model of oil and gas generation, cracking and expulsion. Org. Geochem. 19 (1–3), 161–172. [https://doi.org/10.1016/0146-6380\(92\)90034-U](https://doi.org/10.1016/0146-6380(92)90034-U).
- Bodnar, R.J., Vityk, M.O., 1994. Interpretation of microthermometric data for H₂O-NaCl fluid inclusions. In: De Vivo, B., Frezzotti, M.L. (Eds.), Fluid Inclusions in Minerals, Methods and Applications. pub. by Virginia Tech, Blacksburg, VA, pp. 117–130.
- Bourdet, J., Pironon, J., Levresse, G., Tritlla, J., 2010. Petroleum accumulation and leakage in a deeply buried carbonate reservoir, Níspero field (Mexico). Mar. Petrol. Geol. 27, 126–142. <https://doi.org/10.1016/j.marpetgeo.2009.07.003>.
- Bouster, C., Vermande, P., Veron, J., 1980. Study of the pyrolysis of polystyrenes: I. Kinetics of thermal decomposition. J. Anal. Appl. Pyrol. 1 (4), 297–313. [https://doi.org/10.1016/0165-2370\(80\)80014-3](https://doi.org/10.1016/0165-2370(80)80014-3).
- Burnham, A.K., Braun, R.L., Coburn, T.T., Sandvik, E.I., Curry, D.J., Schmidt, B.J., Noble, R.A., 1996. An appropriate kinetic model for well-preserved algal kerogens. Energy Fuels 10 (1), 49–59. <https://doi.org/10.1021/ef950142s>.
- Burnham, A.K., 1989. A Simple Kinetic Model of Petroleum Formation and Cracking. LLNL Technical Report UCID-21665 ON: DE89008652. Lawrence Livermore National Lab., CA (USA), pp. 1–11.
- Camacho-Ortegón, L.F., 2009. Origine-Evolution-Migration et Stockage, des hydrocarbures dans le bassin de Sabinas, NE Mexique: étude intégrée de pétrographie, géochimie, géophysique et modélisation numérique 1D-2D et 3D. Tesis Doctoral, Faculté des Sciences et Techniques, Université Henri Poincaré, Nancy I, Université de Lorraine, Laboratoire G2R UMR 7566 CNRS, Ecole Doctorale RP2E. UHP - Nancy I, Vandœuvre les Nancy, France, p. 388. NNT : 2009NAN10139, tel-01748331.
- Camacho-Ortegón, L.F., Martínez-Ortegón, L., Pironon, J., Suarez-Ruiz, I., Enciso-Cardenas, J.J., 2017. Modelado del sistema petrolero de la Cuenca de Sabinas,

- Noreste de México ; Parte I: evolución térmica, generación y migración de hidrocarburos. *Bol. Asoc. Mex. Geol. Pet.* LIX (1), 7–46. https://www.researchgate.net/publication/348923459_Modelado_del_sistema_petrolero_de_la_Cuenca_de_Sabina_Noreste_de_Mexico_Parte_1_Evolucion_termica_generacion_y_migracion_de_hidrocarburos_Boletin_de_la_Asoacion_Mexicana_de_Geologos_Petroleros#fullTextFileContent.
- Chávez-Cabello, G., Aranda-Gómez, J.J., Iriando-Perrones, A., 2009. Culminación de la Orogenia Laramide en la Cuenca de Sabinas, Coahuila, México. *Bol. Asoc. Mex. Geol. Pet.* LIV (1), 78–89. http://publicaciones.amgp.org/administrativo/publicaciones/archivos/portada/5dbced90ec0e3_bol.monterrey419mayo1.pdf.
- Clark, K.F., Foster, C.F., Damon, P.E., 1982. Cenozoic mineral deposits and subduction-related arcs in Mexico. *Geol. Soc. Am. Bull.* 93, 533–544. [https://doi.org/10.1130/0016-7606\(1982\)93<533:CMDASM>2.0.CO;2](https://doi.org/10.1130/0016-7606(1982)93<533:CMDASM>2.0.CO;2).
- Cuevas-Leré, J.A., 1985. Analysis of Subsidence and Thermal History in the Sabinas Basin, Northeastern Mexico. University of Arizona, USA, p. 81. M.S. dissertation.
- Dahlen, F.A., Suppe, J., Davis, D., 1984. Mechanics of fold-and-thrust belts and accretionary wedges: cohesive Coulomb theory. *J. Geophys. Res.* 89, 10087–10101. <https://doi.org/10.1029/JB089iB12p10087>.
- Davis, F.A., Engelder, T., 1985. The role of salt in fold-and-thrust belts. *Tectonophysics* 119 (1–4), 67–88. [https://doi.org/10.1016/0040-1951\(85\)90033-2](https://doi.org/10.1016/0040-1951(85)90033-2).
- Demongodin, L., Pinoteau, B., Vasseur, G., Gable, R., 1991. Thermal conductivity and well logs: a case study in the Paris Basin. *Geophys. J. Int.* 105, 675–691. <https://doi.org/10.1111/j.1365-246X.1991.tb00805.x>.
- Dumble, T.E., 1892. Notes on the geology of the valley of the middle Río Grande. *Geol. Soc. Am. Bull.* 3, 219–230. <https://doi.org/10.1130/GSAB-3-219>.
- Eguiluz de Antuñano, S., 2001. Geologic evolution and gas resources of the Sabinas Basin in northeastern Mexico. In: Bartolini, C., Bufler, R.T., Cantú-Chapa, A. (Eds.), *The Western Gulf of Mexico Basin: Tectonics, Sedimentary Basins and Petroleum Systems*, vol. 75. AAPG Memoir, pp. 241–270. <https://doi.org/10.1306/M75768C10>.
- Ewing, T.E., 2003. Review of the tectonic history of the lower Rio Grande border region, south Texas and Mexico, and implications for hydrocarbon exploration. *SIPES Newsl.* 40 (2), 16–21.
- Goldhammer, R.K., Johnson, C.A., 2001. Middle Jurassic-Upper Cretaceous paleogeographic evolution and sequence stratigraphic framework of the Northwest Gulf of Mexico rim. In: Bartolini, C., Bufler, R.T., Cantú-Chapa, A. (Eds.), *The Western Gulf of Mexico Basin: Tectonics, Sedimentary Basins and Petroleum Systems*, vol. 75. AAPG Memoir, pp. 45–81. <https://doi.org/10.1306/M75768C3>.
- Goldhammer, R.K., Lehmann, P.J., Todd, R.G., Wilson, J.L., Ward, W.C., Johnson, C.R., 1991. Sequence Stratigraphy and Cyclostratigraphy of the Mesozoic of Sierra Madre Oriental, Northeast Mexico: a Field Guidebook. Gulf Coast Section, Society of Paleontologists and Mineralogists Foundation, p. 85.
- Gonçalves, F.T.T., Mora, C.A., Córdoba, F., Kairuz, E.C., Giraldo, B.N., 2002. Petroleum generation and migration in the Putumayo Basin, Colombia: insights from an organic geochemistry and basin modelling study in the foothills. *Mar. Petrol. Geol.* 19 (6), 711–725. [https://doi.org/10.1016/S0264-8172\(02\)00034-X](https://doi.org/10.1016/S0264-8172(02)00034-X).
- González-García, R., Holguín-Quiñones, N., 1992. Las rocas generadoras de México. *Bol. Asoc. Mex. Geol. Pet.* 42, 16–30.
- González-Partida, E., Carrillo-Chávez, A., Grimmer, J.O.W., Pironon, J., Mutterer, J., Levresse, G., 2003. Fluorite deposits at Encantada-Buenavista, Mexico: products of Mississippi Valley type processes. *Ore Geol. Rev.* 23 (3–4), 107–124. [https://doi.org/10.1016/S0169-1368\(03\)00018-0](https://doi.org/10.1016/S0169-1368(03)00018-0).
- Gray, G.G., Pottorf, R.J., Yurewicz, D.A., Mahon, K.I., Pevear, D.R., Chuchla, R.J., 2001. Thermal and chronological record of syn- to post-Laramide burial and exhumation, Sierra Madre Oriental, Mexico. In: Bartolini, C., Bufler, R.T., Cantú-Chapa, A. (Eds.), *The Western Gulf of Mexico Basin: Tectonics, Sedimentary Basins and Petroleum Systems: AAPG Memoir*, vol. 75, pp. 159–181. <https://doi.org/10.1306/M75768C7>.
- Handhal, A.M., Mahdi, M.M., 2016. Basin modeling analysis and organic maturation for selected wells from different oil fields, Southern Iraq. *Model. Earth Syst. Environ.* 2, 1–14. <https://doi.org/10.1007/s40808-016-0247-y>.
- Haq, B.U., Hardenbol, J., Vail, P.R., 1987. Chronology of fluctuating sea levels since the Triassic. *Science* 235, 1156–1167. <https://doi.org/10.1126/science.235.4793.1156>.
- Heim, A., 1926. Notes on the Jurassic of Tamazunchale Sierra Madre oriental, Mexico. *Eclogae Geol. Helv.* 20, 84–87. <https://doi.org/10.5169/seals-158600>.
- Humphrey, W.E., 1949. Geology of the Sierra de los Muertos area, Mexico (with Descriptions of Aiptian Cephalopods from the La Peña Formation). *Bull. Geol. Soc. Am.* 60, 89–176. [https://doi.org/10.1130/0016-7606\(1949\)60\[89:GOTSDDL\]2.0.CO;2](https://doi.org/10.1130/0016-7606(1949)60[89:GOTSDDL]2.0.CO;2).
- Humphrey, W.E., Díaz, T., 1956. Jurassic and Lower Cretaceous Stratigraphy and Tectonics of Northeast Mexico. PEMEX file, NE-M-799, pp. 25–35.
- Imlay, R., 1936. Geology of the western part of the Sierra de Parras. *Geol. Soc. Am. Bull.* 47, 1091–1152. <https://doi.org/10.1130/GSAB-47-1091>.
- Imlay, R., 1937. Geology of the middle part of the Sierra Parras. *Geol. Soc. Am. Bull.* 48, 587–630. <https://doi.org/10.1130/GSAB-48-587>.
- Imlay, R.W., 1940. Neocomian Fauna of northern Mexico. *Geol. Soc. Am. Bull.* 51, 117–190. <https://doi.org/10.1130/GSAB-51-117>.
- ISO 7404-3, 1994. Methods for the Petrographic Analysis of Bituminous Coal and Anthracite, Part 3: Method of Determining Maceral Group Composition. International Organization for Standardization, Geneva, Switzerland, p. 6.
- ISO 7404-5, 1994. Methods for the Petrographic Analysis of Bituminous Coal and Anthracite, Part 5: Method of Determining Microscopically the Reflectance of Vitrinite. International Organization for Standardization, Geneva, Switzerland, p. 12.
- Kelly, A.W., 1936. Evolution of the Coahuila Peninsula, Mexico, part II, geology of the mountains bordering the valleys of acatita and las Delicias. *Geol. Soc. Am. Bull.* 47, 1009–1039. <https://doi.org/10.1130/GSAB-47-1009>.
- Lawton, T.F., Vega-Vera, F.J., Giles, K.A., Rosales-Domínguez, C., 2001. Stratigraphy and origin of the La Popa basin, Nuevo leon and Coahuila, Mexico. In: Bartolini, C., Bufler, R.T., Cantú-Chapa, A. (Eds.), *The Western Gulf of Mexico Basin: Tectonics, Sedimentary Basins and Petroleum Systems*, vol. 75. AAPG Memoir, pp. 219–240. <https://doi.org/10.1306/M75768C9>.
- Longoria, F.J., 1984. Stratigraphic studies in the Jurassic of northeastern Mexico: evidence for the origin of Sabinas Basin. In: *The Jurassic of the Gulf Rim: Gulf Coastal Section, Society for Sedimentary Geology (SEPM) Foundation, Third Annual Research Conference Proceedings*, pp. 171–193.
- McBride, E.F., Caffey, K.C., 1979. Geologic report on upper Cretaceous coal-bearing rocks, Rio Escondido basin, Coahuila, Mexico. *Bol. Asoc. Mex. Geol. Pet.* 40, 21–47.
- Márquez, B., 1979. Evaluación petrolera de sedimentos carbonatados del Cretácico en el Golfo de Sabinas, NE de México. *Rev. Ing. Petrol.* 19 (8), 28–36.
- Marret, R., Aranda, G.M., 1999. Structure and kinematic development of the Sierra Madre Oriental fold-thrust belt, Mexico. In: *South Texas Geological Society Field Trip, Stratigraphy and Structure of the Jurassic and Cretaceous Platform and Basin Systems of the Sierra Madre Oriental*, pp. 69–98.
- Martínez, L., Duplay, J., Suarez-Ruiz, I., Disnar, J.R., Farjanel, G., Larqué, P., Liewig, N., 2002. Evolution thermique des séries sédimentaires de la Marge ardéchoise: étude pétrographique de la matière organique et des argiles (Thermal evolution of the sedimentary series of the Ardèche Margin: petrological studies of organic matter and clays). *Compt. Rendus Geosci.* 334 (14), 1021–1028. [https://doi.org/10.1016/S1631-0713\(02\)01848-5](https://doi.org/10.1016/S1631-0713(02)01848-5).
- Mello, U.T., Karner, G.D., Anderson, R.N., 1995. Role of salt in restraining the maturation of subsalt rocks. *Mar. Petrol. Geol.* 12 (7), 697–716. [https://doi.org/10.1016/0264-8172\(95\)93596-V](https://doi.org/10.1016/0264-8172(95)93596-V).
- Morton-Bermea, O., 1995. Petrologie, Mineralogie und Geochemie des Alkali-Intrusivkomplexes von Monclova-Candela (Mexiko). Deutschland, Universität Hamburg [Doktorgrade], p. 100.
- Morton-Bermea, O., 1997. Magmatism of the northern Gulf of Mexico alkaline province (Sierra de Picachos and Monclova-Candela belt). In: *American Geophysical Union, Fall Meeting, San Francisco, CA, USA. Eos, Transactions. AGU*, vol. 78, p. F823. No. 48.
- Murillo-Muñeton, G., 1999. Stratigraphic Architecture, Platform Evolution, and Mud-Mound Development in the Lower Cupido Formation (Lower Cretaceous), Northeastern Mexico. Doctoral thesis. Texas A&M University, College Station, p. 53.
- Pepper, A.S., Corvi, P.J., 1995. Simple kinetic models of petroleum generation. Part I: oil and gas generation from kerogen. *Mar. Petrol. Geol.* 12 (3), 291–319. [https://doi.org/10.1016/0264-8172\(95\)98381-E](https://doi.org/10.1016/0264-8172(95)98381-E).
- Petromod, 2D, 2007. PetroMod 2D Basic Tutorial. IES GmbH Integrated Exploration Systems. Aachen Germany. Version 10, Rev. A, p. 97.
- Piedad-Sánchez, N., 2004. Prospección de hidrocarburos par une approche intégrée de pétrographie, géochimie et modélisation de la transformation de la matière organique: analyse et reconstitution de l'histoire thermique des Bassins Carbonifère Central des Asturies (Espagne) et Sabinas-Piedras Negras (Coahuila, Mexique). Doctoral thesis. UHP Nancy I, France, p. 356.
- Pironon, J., 2004. Fluids Inclusions in petroleum environments; analytical procedure for PTX reconstruction. *Acta Petrol. Sin.* 20 (6), 1333–1342. http://en.igg-journals.cn/article/id/aps_200406131, 2004.
- Price, J.C., Henry, C.D., 1984. Stress orientations during Oligocene volcanism in Trans-Pecos, Texas: timing the transition from Laramide compression to basin and range tension. *Geology* 12, 238–241. [https://doi.org/10.1130/0091-7613\(1984\)12<238:SODOVI>2.0.CO;2](https://doi.org/10.1130/0091-7613(1984)12<238:SODOVI>2.0.CO;2).
- Ritzwoller, M.H., Shapiro, N.M., 2001. Lithospheric inversions and the assimilation of complementary information: some examples relevant for Earth Scope. In: *Proceedings of the Earth Scope Workshop. Snowbird, Utah*, pp. 383–387.
- Roedder, E., 1984. Fluid inclusions. *Mineral. Soc. Am. Rev. Mineral.* 12, 644.
- Román-Ramos, J.R., Holguín-Quiñones, N., 2001. Subsistemas generadores de la región norte de México. *Bol. Asoc. Mex. Geol. Pet.* 49, 68–84.
- Sachsenhofer, R.F., 2001. Syn- and post-collisional heat flow in the Cenozoic eastern Alps. *Int. J. Earth Sci.* 90, 579–592. <https://doi.org/10.1007/s005310000179>.
- Santamaría-Orozco, D., Ortuño, F., Adatte, T., Ortiz, A., Riba, A., Franco, S., 1991. Evolución geodinámica de la Cuenca de Sabinas y sus implicaciones petroleras. Estado de Coahuila. Instituto Mexicano del Petróleo, p. 209. Tomo I, CAO-3508 Internal report.
- Schegg, R., Cornford, C., Werner, L.M., 1999. Migration and accumulation of hydrocarbons in the Swiss Molasse Basin: implications of a 2D basin modelling study. *Mar. Petrol. Geol.* 16 (6), 511–531. [https://doi.org/10.1016/S0264-8172\(99\)00018-5](https://doi.org/10.1016/S0264-8172(99)00018-5).
- Sweeney, J.J., Burnham, A.K., 1990. Evaluation of a simple model of vitrinite reflectance based on chemical kinetics. *AAPG (Am. Assoc. Pet. Geol.) Bull.* 74, 1559–1570. <https://doi.org/10.1306/0C9B251F-1710-11D7-8645000102C1865D>.
- Taylor, G.H., Teichmüller, M., Davis, A., Diessel, C.F.K., Littke, R., Robert, P., 1998. *Organic Petrology*. Schweizerbart Science Publishers, Stuttgart, Germany, p. 704.
- Tissot, B.P., Welte, D.H., 1984. *Petroleum Formation and Occurrence*, 2 edn. Springer, New York, p. 699. <https://doi.org/10.1007/978-3-642-87813-8>.
- Tobin, R.C., Claxton, B.L., 2000. Multidisciplinary thermal maturity studies using vitrinite reflectance and fluid inclusion microthermometry: a new calibration of old techniques. *Ame. Assoc. Petrol. Geol.* 84 (10), 1647–1665. <https://doi.org/10.1306/8626BF29-173B-11D7-8645000102C1865D>.
- Ungerer, P., Pelet, R., 1987. Extrapolation of kinetics of oil and gas formation from laboratory experiments to sedimentary basins. *Nature* 327, 52–54. <https://doi.org/10.1038/327052a0>.
- Vail, P.R., Mitchum, R.M., Thompson, S., 1977. Seismic stratigraphy and global changes of sea-level, IV. Global cycles of relative changes of sea-level. In: *Payton, C. (Ed.), Seismic Stratigraphy-Applications to Hydrocarbon Exploration*. American

- Association Petroleum Geologists, Memoir, vol. 26, pp. 83–97. <https://doi.org/10.1306/M26490>.
- Van Balen, R.T., Van Bergen, F., De Leeuw, C., Pagnier, H., Simmelink, H., Van Wees, J. D., Verweij, J.M., 2000. Modelling the hydrocarbon generation and migration in the West Netherlands Basin, The Netherlands. *Geol. Mijnbouw/Netherlands J. Geosci.* 79, 29–44. <https://doi.org/10.1017/S0016774600021557>.
- Vandenbroucke, M., Behar, F., Rudkiewicz, J.L., 1999. Kinetic modelling of petroleum formation and cracking: implications from the high pressure/high temperature Elgin Field (UK, North Sea). *Org. Geochem.* 30 (9), 1105–1125. [https://doi.org/10.1016/S0146-6380\(99\)00089-3](https://doi.org/10.1016/S0146-6380(99)00089-3).
- Wan Hasiah, A., 2001. Suberinite - bituminite and phlobaphinite - inertinite associations in the oil - generating coals of Northwest Borneo. In: Petersen, H.I. (Ed.), Abstracts of the Society for Organic Petrology (TSOP)/International Committee for Coal and Organic Petrology (ICCP). The 53rd Meeting of the International Committee for Coal and Organic Petrology, pp. 146–151. Copenhagen, Denmark.
- Walderhaug, O., 1990. A fluid inclusion study of quartz-cemented sandstones from offshore mid-Norway—possible evidence for continued quartz cementation during oil emplacement. *J. Sediment. Petrol.* 60, 203–210. <https://doi.org/10.1306/212F9151-2B24-11D7-8648000102C1865D>.
- Wilson, J.L., 1990. Basement structural controls on Mesozoic carbonate facies in Northeastern Mexico - a review. In: Tucker, M.E., Wilson, J.L., Crevello, P.D., Sarg, J. R., Read, J.F. (Eds.), *Carbonate Platforms, Facies, Sequences and Evolution: International Association of Sedimentologists*, vol. 9. Special Publication, pp. 235–255.
- Zeman, A., Suchy, V., Stejskal, M., Janku, J., Cermak, J., Turek, K., 2000. Migration of fluids controlled by equidistant fracture systems: an example from Central Europe (Czech Republic, Slovakia and Austria). *J. Geochem. Explor.* 69–70, 499–504. [https://doi.org/10.1016/S0375-6742\(00\)00035-2](https://doi.org/10.1016/S0375-6742(00)00035-2).